# Chaotic dynamics and resonant effects in near-Earth orbital motion


Haris Skokos

Nonlinear Dynamics and Chaos (NDC) group
Department of Mathematics and Applied Mathematics
University of Cape Town, South Africa

E-mail: haris.skokos@uct.ac.za, haris.skokos@gmail.com
URL: http://math_research.uct.ac.za/~hskokos/


Workshop 'Chaos and Nonlinearity in Dynamical Astronomy'
Institute for Fundamental Physics of the Universe, Trieste, Italy, 24 February 2026


Work supported by the National Research Foundation (NRF) of South Africa
(reference number WABR240401211578)


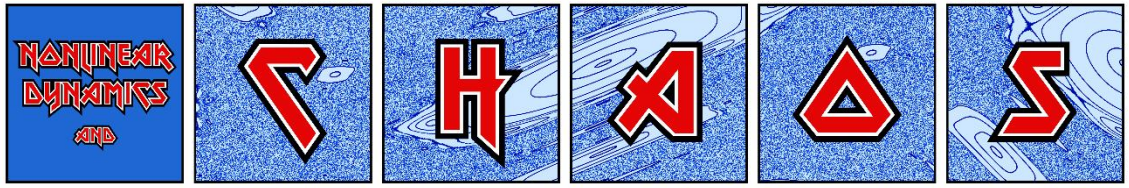


# Work in collaboration with

**Cassandra Barbis**

MSc student, University of Cape Town, South Africa

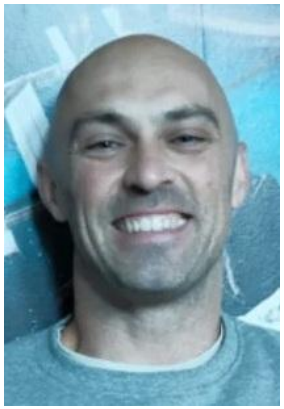

**Jérôme Daquin**

Centre de Physique Théorique, Luminy Campus, Marseille, France & Université de Toulon, Toulon, France

**Elisa Maria Alessi**

Istituto di Matematica Applicata e Tecnologie Informatiche "E. Magenes", Milan, Italy

# University of Cape Town (UCT)

# University of Cape Town (UCT)

# Cape Town

# Outline

- Motivation and problem statement:
  In the context of the space debris problem, we extend previous studies by investigating how the coupled effect of solar radiation pressure (SRP) and Earth's oblateness (J2) can drive chaotic eccentricity growth and enable passive debris reentry.
- Hamiltonian system:
  Perturbations of the two-body problem due to SRP and Earth's oblateness effect.
- Chaos detection:
  The Smaller ALignment Index (SALI).
- Parametric cartography and numerical investigations:
  SALI and orbital lifetime.
- Summary.

# The Hamiltonian model

# Hamiltonian model

Following Alessi et al., MNRAS (2018) and Gkolias et al., Celest. Mech. Dyn. Astron. (2020) the motion of a satellite (mass $m$) around Earth (mass $m_E$, radius $r_E$) is described by a perturbed two-body secular Hamiltonian where the Earth's oblateness ($J_2$) and the solar radiation pressure (SRP) are taken into account:

$$\bar{\mathcal{H}} = \frac{(r_E^2 J_2 \mu^4)\left(G^2 - 3H^2\right)}{4G^5L^3} - \frac{3(c_R P \frac{A}{m})L^2}{2\mu}\sqrt{1-\frac{G^2}{L^2}}\sum_{k=1}^{6}\mathcal{T}_k \cos\psi_k + n_S J.$$

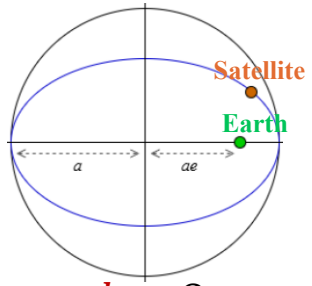


We use Delaunay variables

$$L = \sqrt{g(m_E+m)a}, \qquad l = M, \qquad G = L\sqrt{1-e^2}, \qquad g = \omega, \qquad H = G\cos i\,, \qquad h = \Omega,$$

related to the orbital elements $a$ (semi-major axis), $e$ (eccentricity), $i$ (inclination), $\Omega$ (longitude of node), $\omega$ (argument of perigee), and $M(t) = \sqrt{g(m_E+m)a^{-3/2}}(t-t_0)$ (mean anomaly), with $g$ being the gravitational constant, $t$ is time and $t_0$ the time at which the satellite is closest to Earth.

We also have $J_2 = 0.0010826$ (oblateness parameter), $\mu = gm_E$ (Earth's gravitational parameter), $c_R = 1$ (reflectivity coefficient), $P = 4.56 \times 10^{-6}$ (SRP constant at 1 AU), $A/m$ the area-to-mass ratio, $\varepsilon = 23.4°$(ecliptic's obliquity) and $\lambda_\odot = \lambda_{\odot,0} + n_S t$ is the Sun's ecliptic longitude in terms of the Sun's mean motion $n_S$.

| $k$ | $\mathcal{T}_k$ | $\cos\psi_k$ |
|---|---|---|
| 1 | $\frac{1}{4}(\cos\varepsilon+1)(\cos i+1)$ | $\cos(\omega+\Omega-\lambda_\odot)$ |
| 2 | $-\frac{1}{4}(\cos\varepsilon+1)(\cos i-1)$ | $\cos(-\omega+\Omega-\lambda_\odot)$ |
| 3 | $\frac{1}{2}\sin i\,\sin\varepsilon$ | $\cos(\omega-\lambda_\odot)$ |
| 4 | $-\frac{1}{2}\sin i\,\sin\varepsilon$ | $\cos(\omega+\lambda_\odot)$ |
| 5 | $-\frac{1}{4}(\cos\varepsilon-1)(\cos i+1)$ | $\cos(\omega+\Omega+\lambda_\odot)$ |
| 6 | $\frac{1}{4}(\cos\varepsilon-1)(\cos i-1)$ | $\cos(-\omega+\Omega+\lambda_\odot)$ |

Note that $l$ is a cyclic coordinate, therefore $L$ and $a$ are constants. We eliminate the system's explicit time dependency by introducing the dummy action $J$ with frequency $n_s$, thereby obtaining an autonomous system with 3 degrees of freedom.

# The Smaller ALignment Index (SALI) method of chaos detection

# Maximum Lyapunov Exponent (MLE)

Chaos: sensitive dependence on initial conditions.

Roughly speaking, the MLE of a given orbit characterizes the mean exponential rate of divergence of trajectories surrounding it.

Consider an orbit in the *2N*-dimensional phase space with initial condition *x(0)* and an initial deviation vector *v(0)* (small perturbation) from it.
Then the mean exponential rate of divergence is:

$$MLE = \lambda_1 = \lim_{t\to\infty} \Lambda(t) = \lim_{t\to\infty} \frac{1}{t} ln \frac{\|v(t)\|}{\|v(0)\|}$$

$\lambda_1 = 0 \rightarrow$ Regular motion ($\Lambda \propto t^{-1}$)

$\lambda_1 > 0 \rightarrow$ Chaotic motion

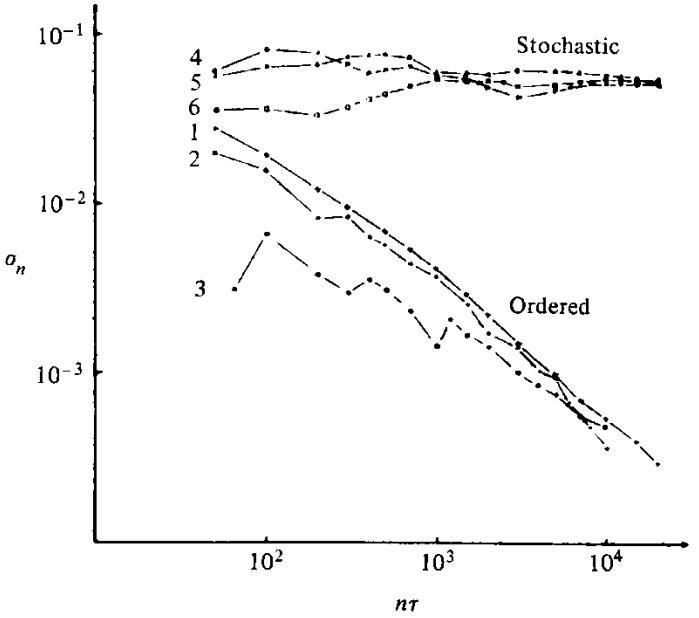


Figure 5.7. Behavior of $\sigma_n$ at the intermediate energy $E = 0.125$ for initial points taken in the ordered (curves 1–3) or stochastic (curves 4–6) regions (after Benettin *et al.*, 1976).

# Definition of the SALI

We follow the evolution in time of two different initial deviation vectors ($v_1(0)$, $v_2(0)$), and define SALI [S., J. Phys. A (2001) – S. & Manos, Lect. Notes Phys. (2016)] as:

$$SALI(t) = min\{\|\hat{v}_1(t) + \hat{v}_2(t)\|, \|\hat{v}_1(t) - \hat{v}_2(t)\|\}$$

where

$$\hat{v}_1(t) = \frac{v_1(t)}{\|v_1(t)\|}$$

When the two vectors become collinear

$$SALI(t) \rightarrow 0$$

# Behavior of SALI for chaotic motion

For chaotic orbits the two initially different deviation vectors tend to coincide with the direction defined by the maximum Lyapunov exponent.

# Behavior of SALI for chaotic motion

For chaotic orbits the two initially different deviation vectors tend to coincide with the direction defined by the maximum Lyapunov exponent.

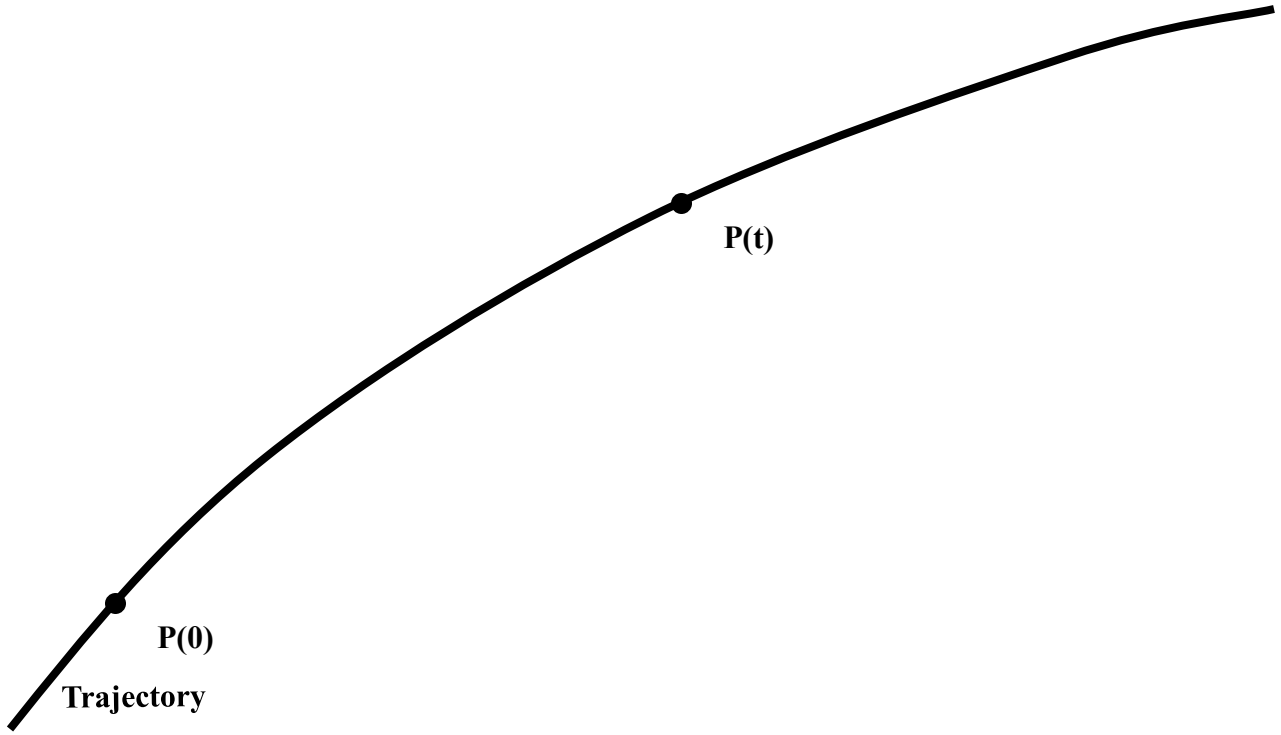

# Behavior of SALI for chaotic motion

For chaotic orbits the two initially different deviation vectors tend to coincide with the direction defined by the maximum Lyapunov exponent.

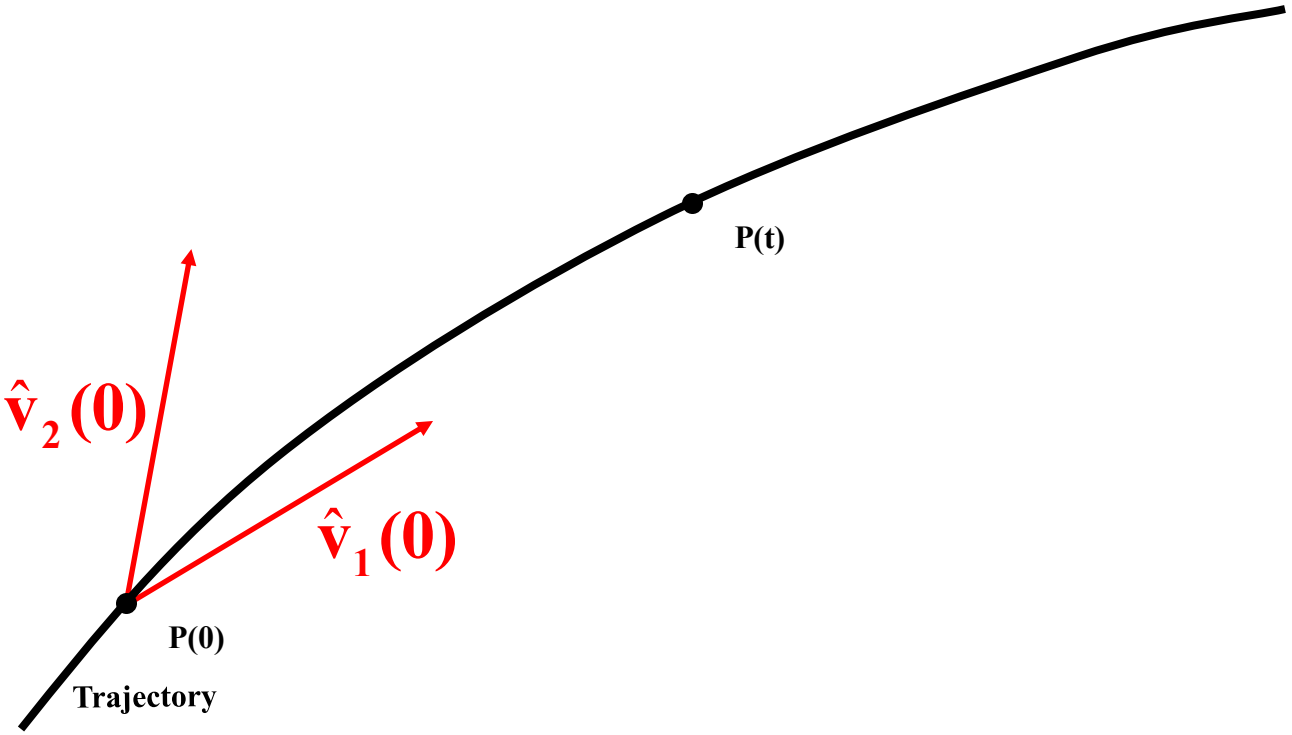

# Behavior of SALI for chaotic motion

For chaotic orbits the two initially different deviation vectors tend to coincide with the direction defined by the maximum Lyapunov exponent.

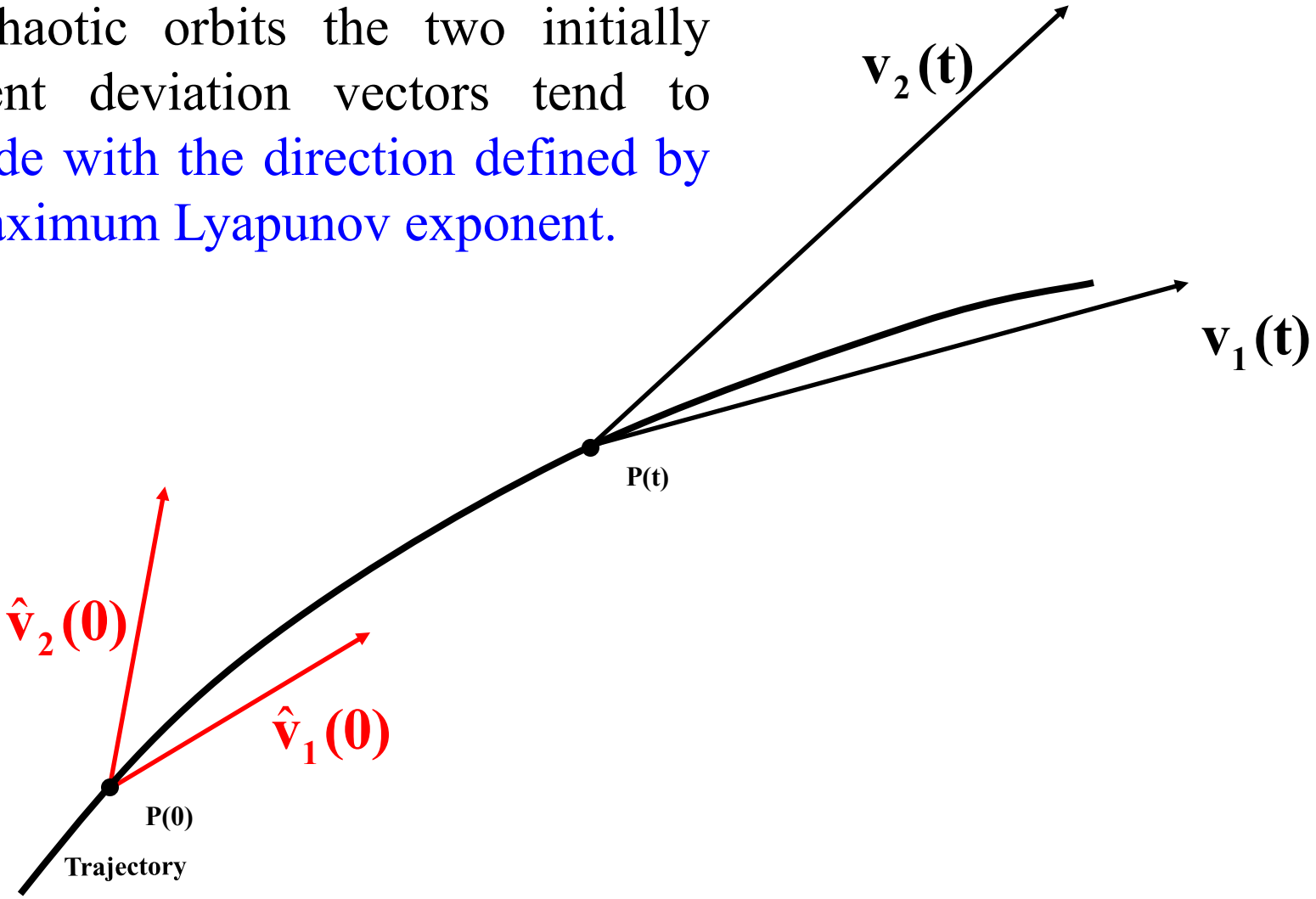

# Behavior of SALI for chaotic motion

For chaotic orbits the two initially different deviation vectors tend to coincide with the direction defined by the maximum Lyapunov exponent.

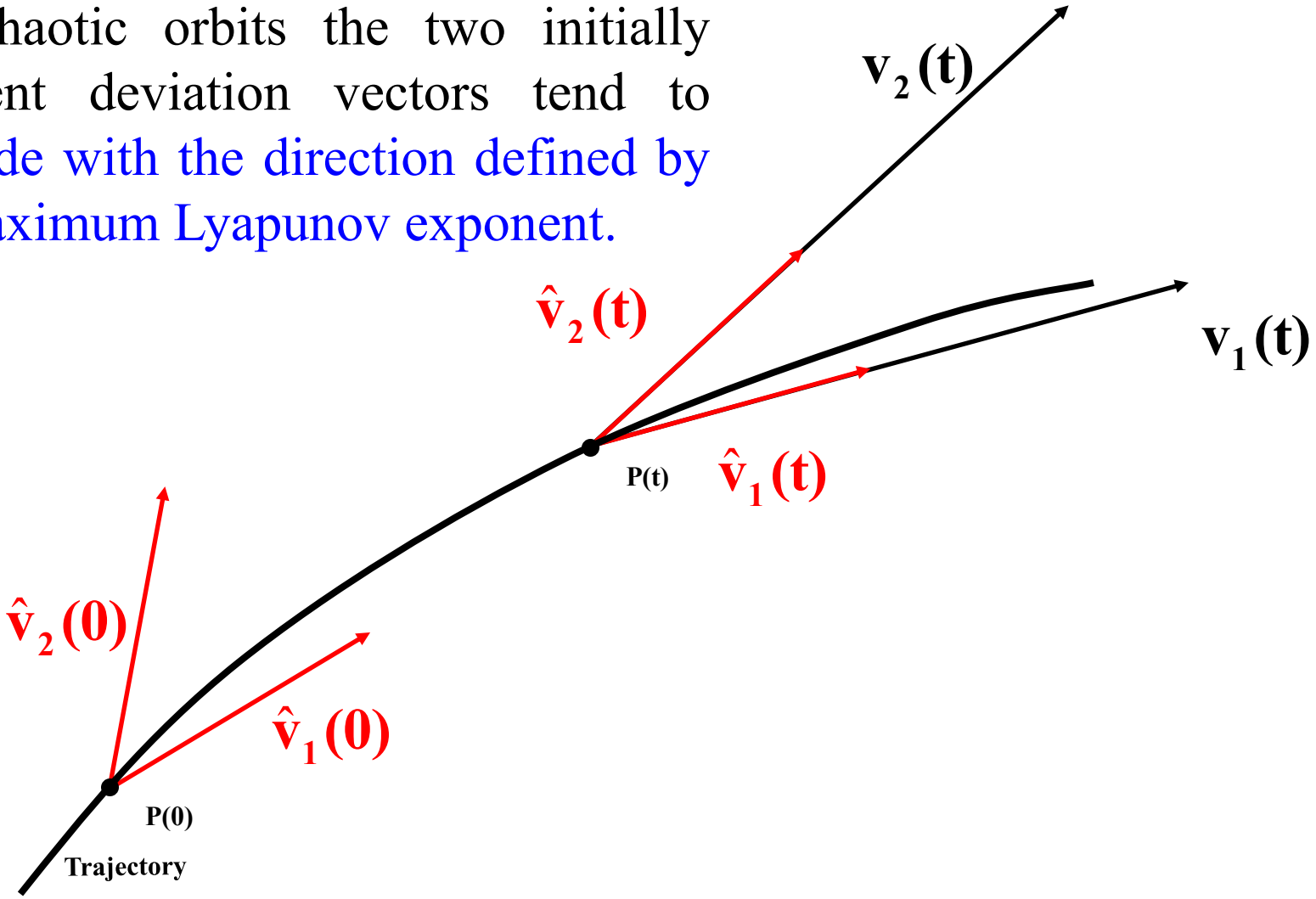

# Behavior of SALI for chaotic motion

For chaotic orbits the two initially different deviation vectors tend to coincide with the direction defined by the maximum Lyapunov exponent.

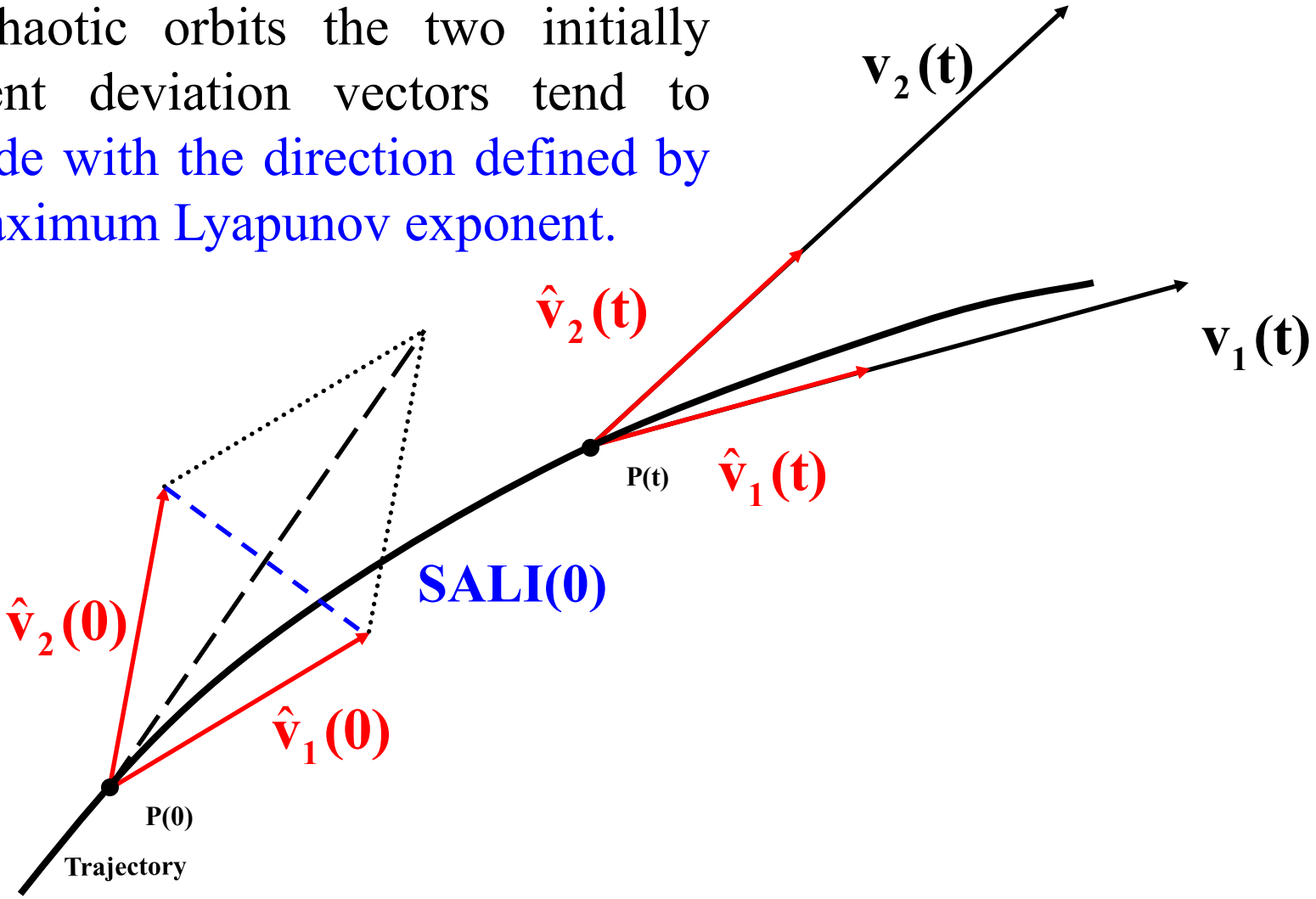

# Behavior of SALI for chaotic motion

For chaotic orbits the two initially different deviation vectors tend to coincide with the direction defined by the maximum Lyapunov exponent.

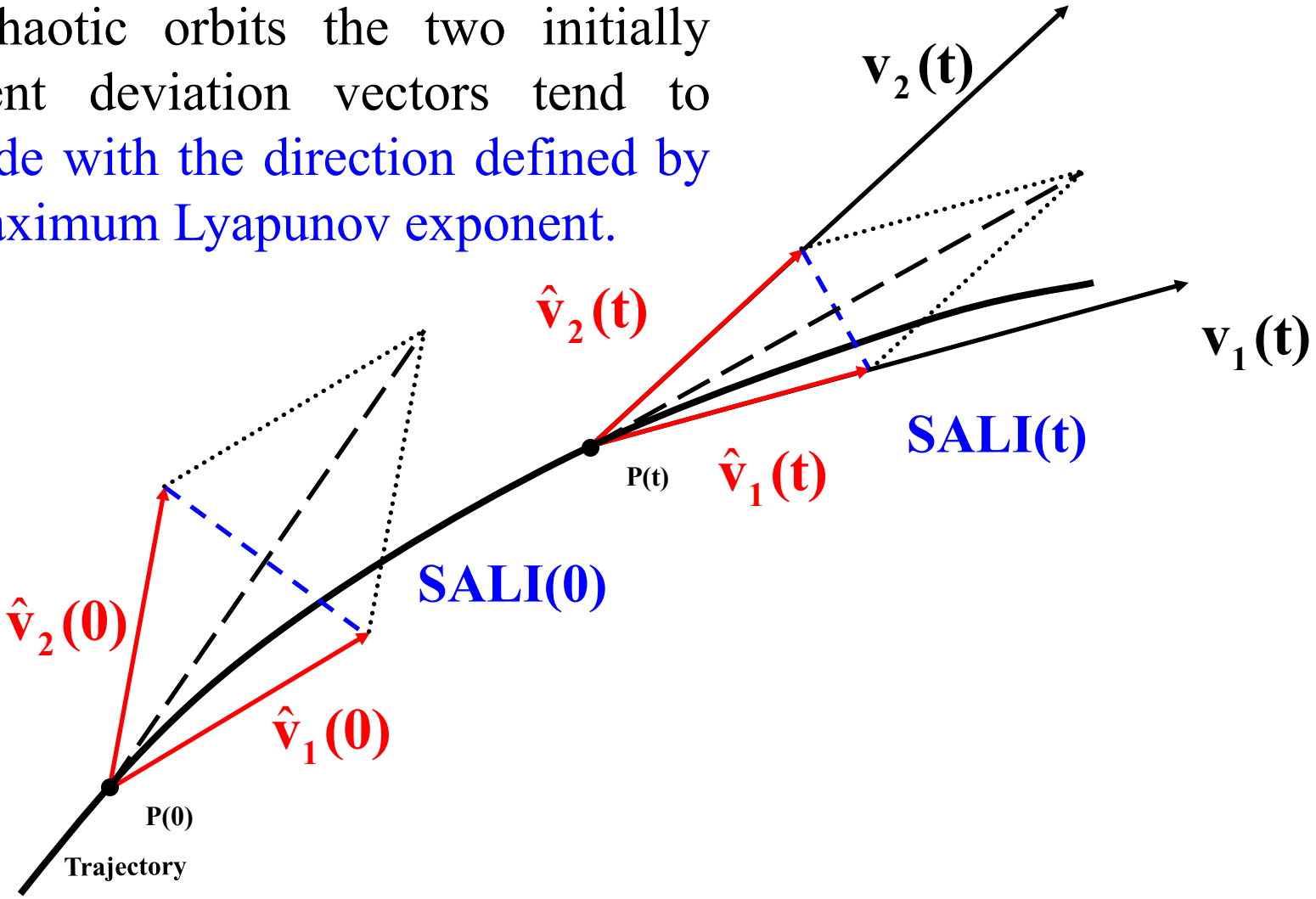

# Behavior of the SALI for chaotic motion

We test the validity of the approximation $SALI \propto e^{-(\lambda_1-\lambda_2)t}$ [S. et al., J. Phys. A (2004)] for a chaotic orbit of the 3D Hamiltonian

$$H = \sum_{i=1}^{3} \frac{\omega_i}{2}(q_i^2 + p_i^2) + q_1^2 q_2 + q_1^2 q_3$$

with $\omega_1$=1, $\omega_2$=1.4142, $\omega_3$=1.7321, H=0.09

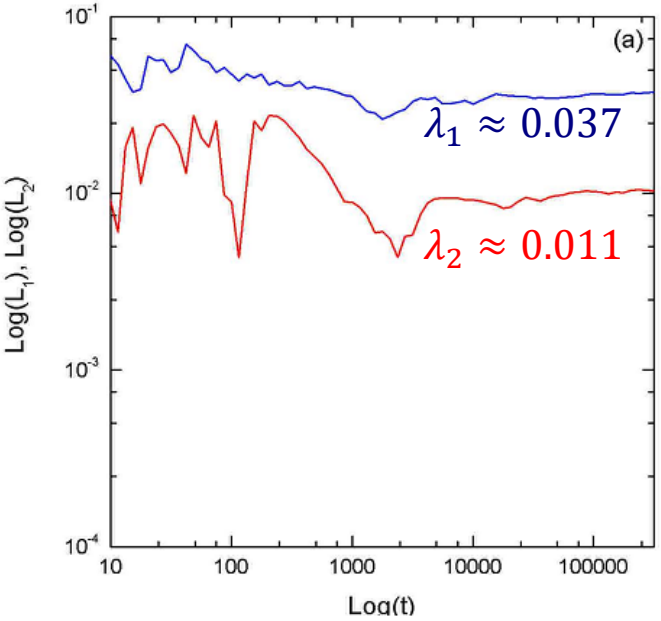


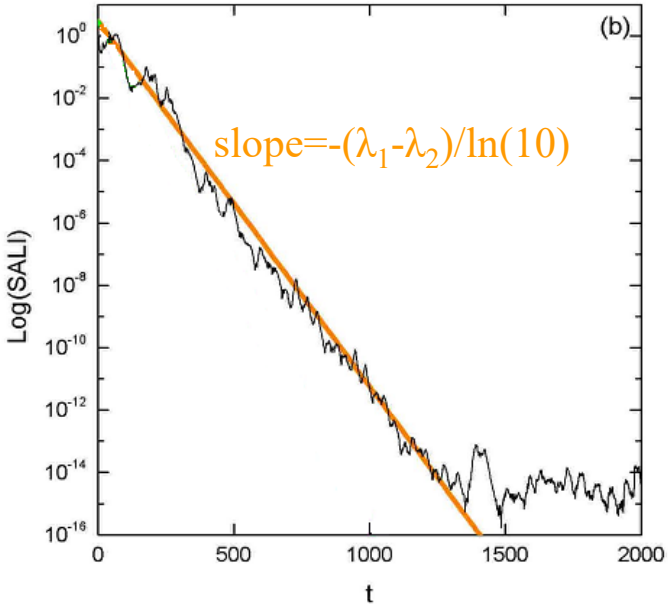

# Behavior of SALI for regular motion

Regular motion occurs on a torus and two different initial deviation vectors become tangent to the torus, generally having different directions.

# Behavior of SALI for regular motion

Regular motion occurs on a torus and two different initial deviation vectors become tangent to the torus, generally having different directions.

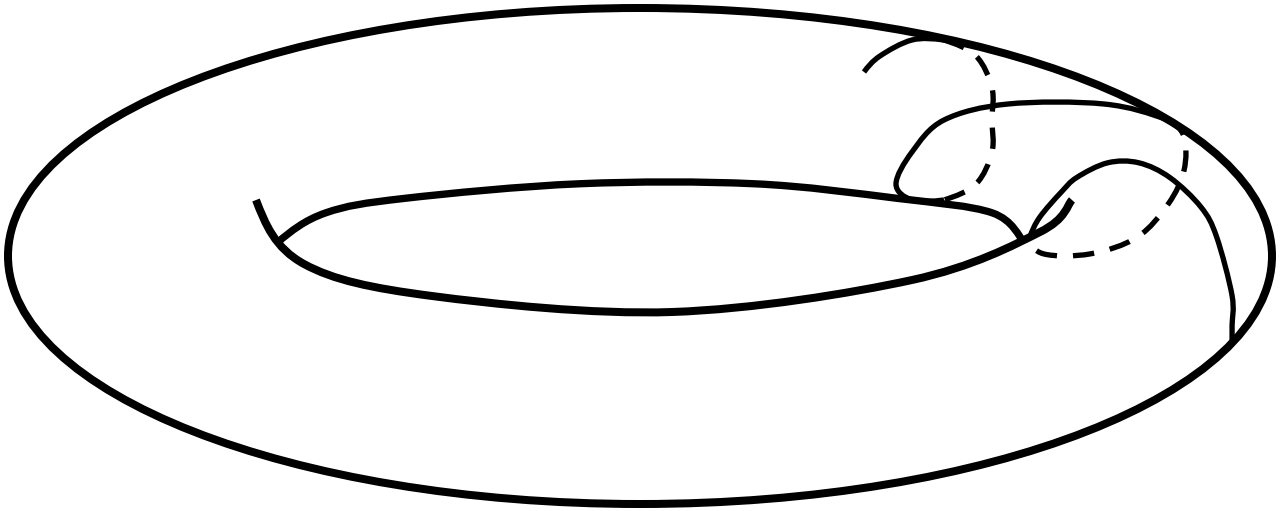

# Behavior of SALI for regular motion

Regular motion occurs on a torus and two different initial deviation vectors become tangent to the torus, generally having different directions.

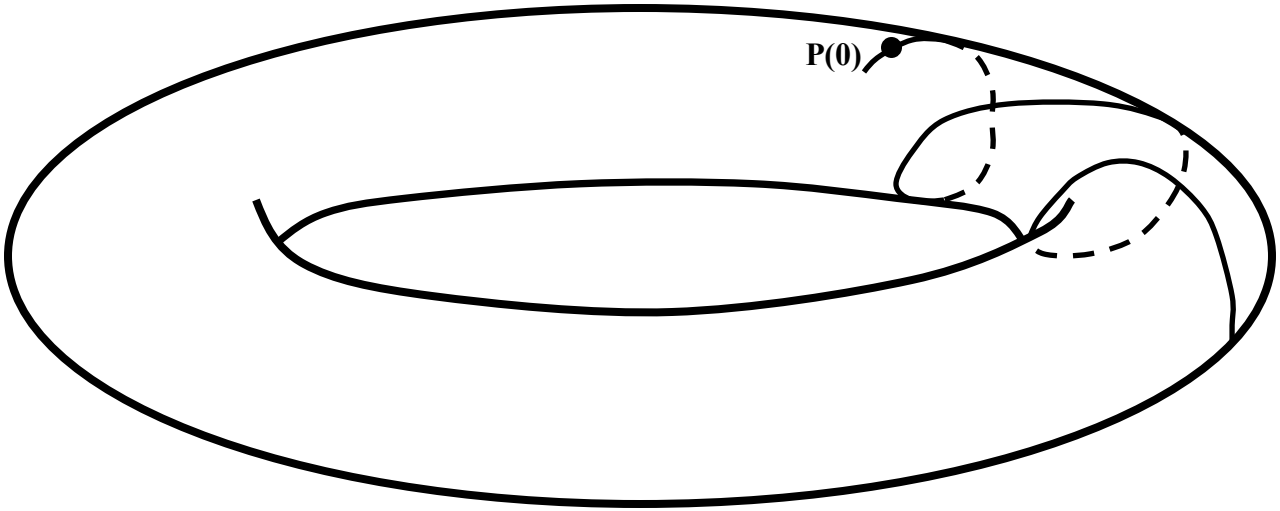

# Behavior of SALI for regular motion

Regular motion occurs on a torus and two different initial deviation vectors become tangent to the torus, generally having different directions.

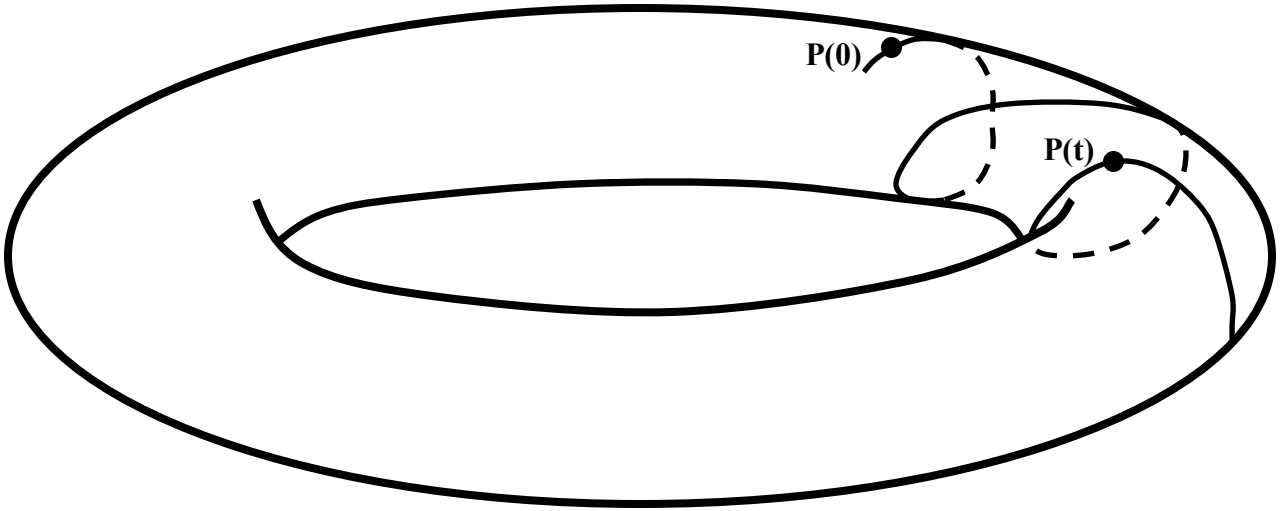

# Behavior of SALI for regular motion

Regular motion occurs on a torus and two different initial deviation vectors become tangent to the torus, generally having different directions.

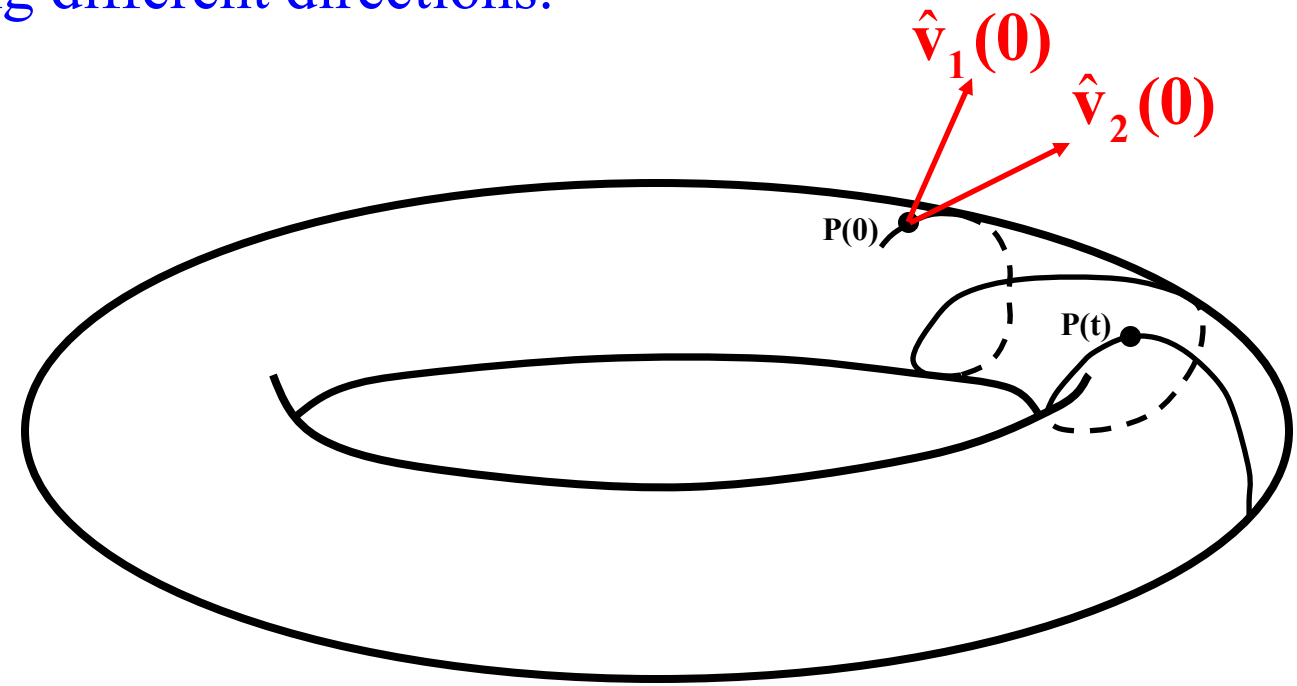

# Behavior of SALI for regular motion

Regular motion occurs on a torus and two different initial deviation vectors become tangent to the torus, generally having different directions.

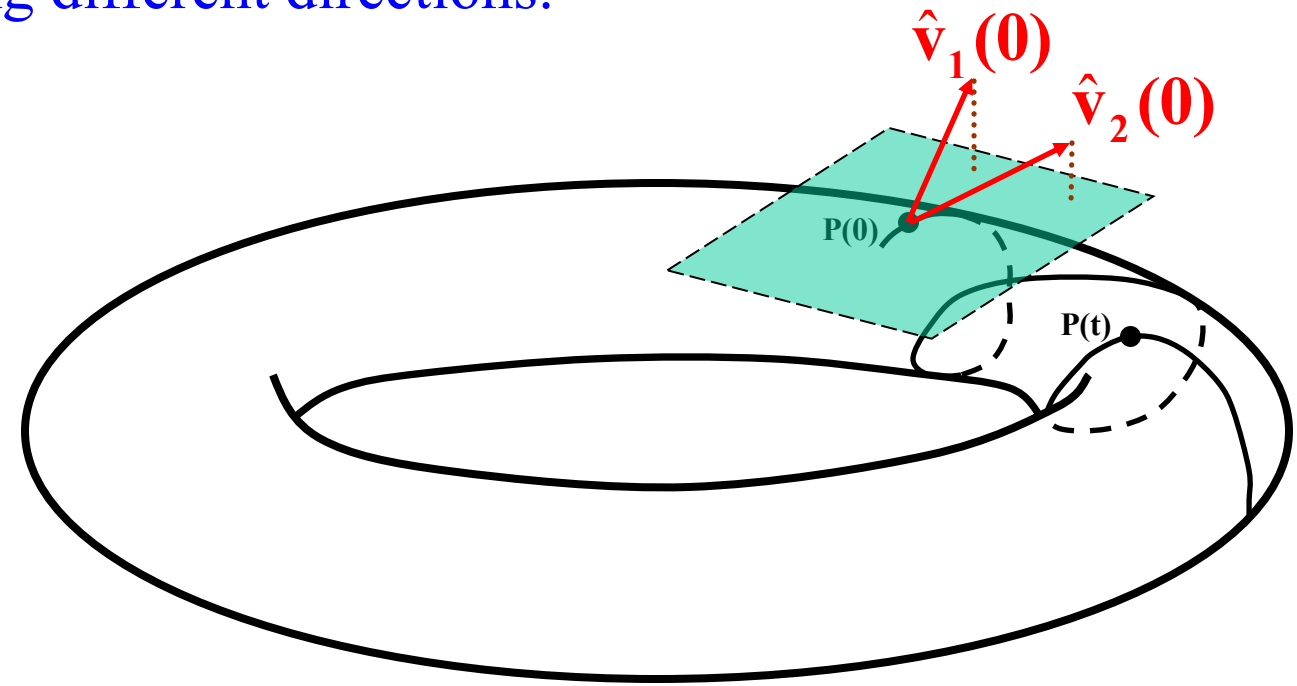

# Behavior of SALI for regular motion

Regular motion occurs on a torus and two different initial deviation vectors become tangent to the torus, generally having different directions.

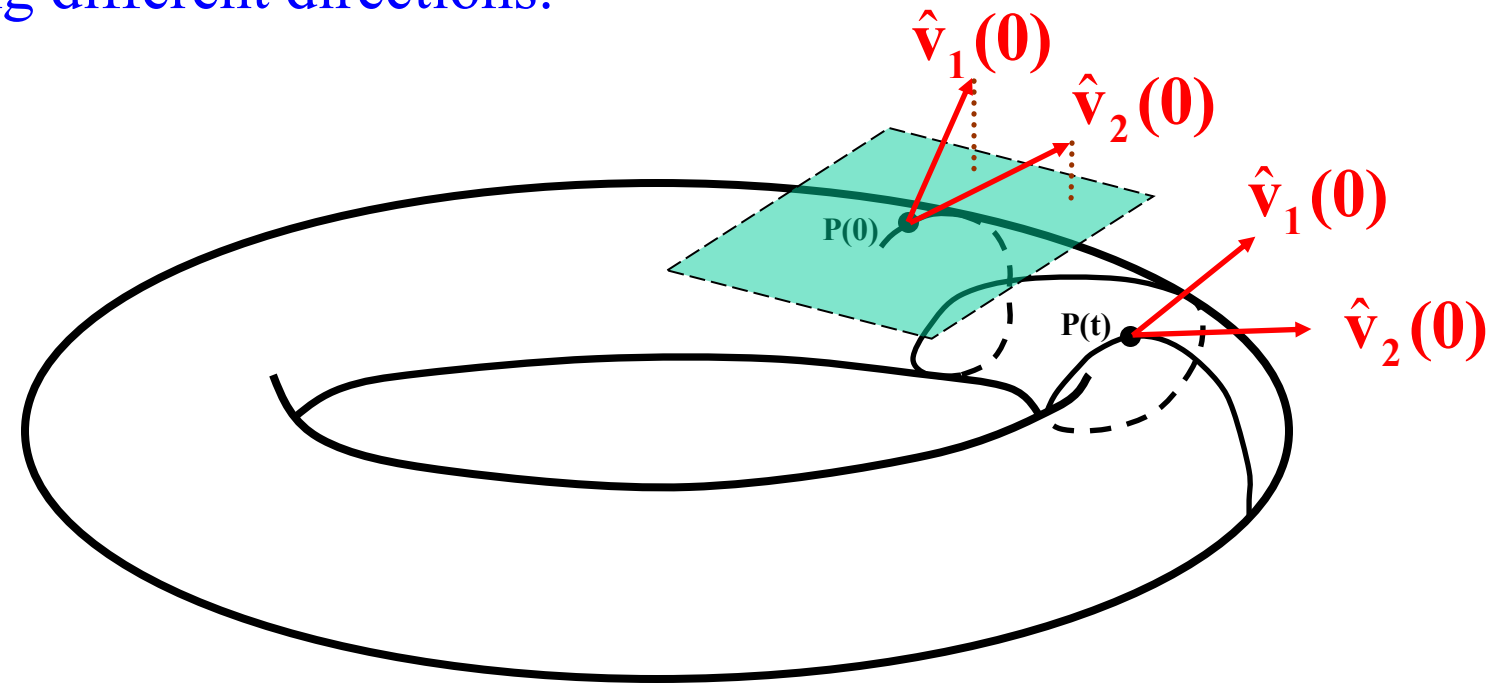

# Behavior of SALI for regular motion

Regular motion occurs on a torus and two different initial deviation vectors become tangent to the torus, generally having different directions.

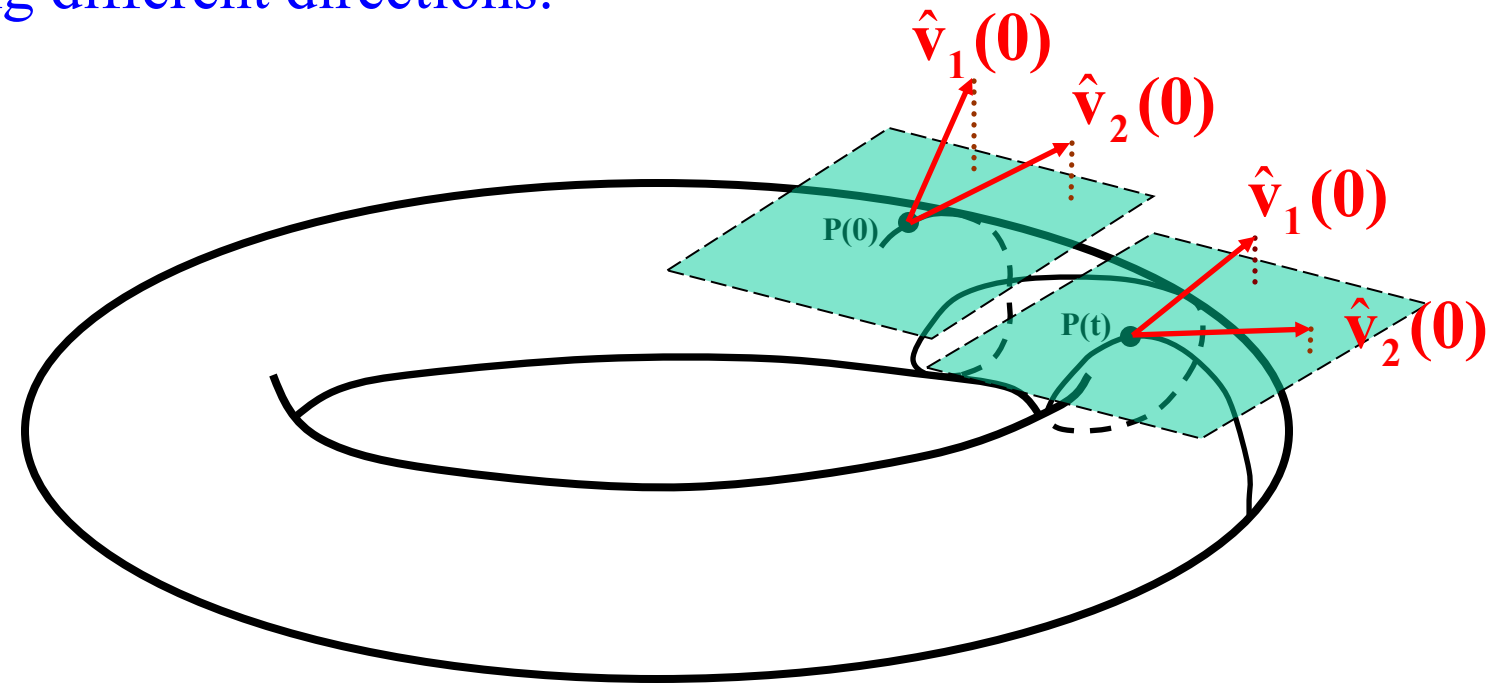

# SALI – Hénon-Heiles system

As an example, we consider the 2D Hénon-Heiles system:

$$H = \frac{1}{2}\left(p_x^2 + p_y^2\right) + \frac{1}{2}\left(x^2 + y^2\right) + x^2 y - \frac{1}{3}y^3$$

For E=1/8 we consider the orbits with initial conditions:
Regular orbit, x=0, y=0.55, $p_x$=0.2417, $p_y$=0
Chaotic orbit, x=0, y=-0.016, $p_x$=0.49974, $p_y$=0
Chaotic orbit, x=0, y=-0.01344, $p_x$=0.49982, $p_y$=0

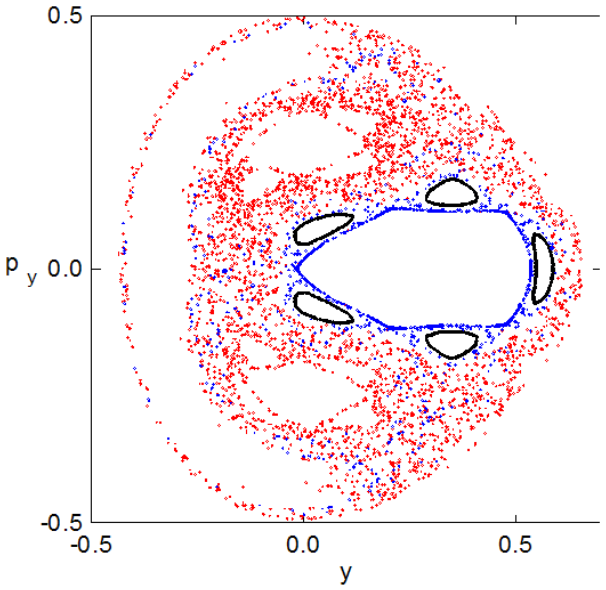


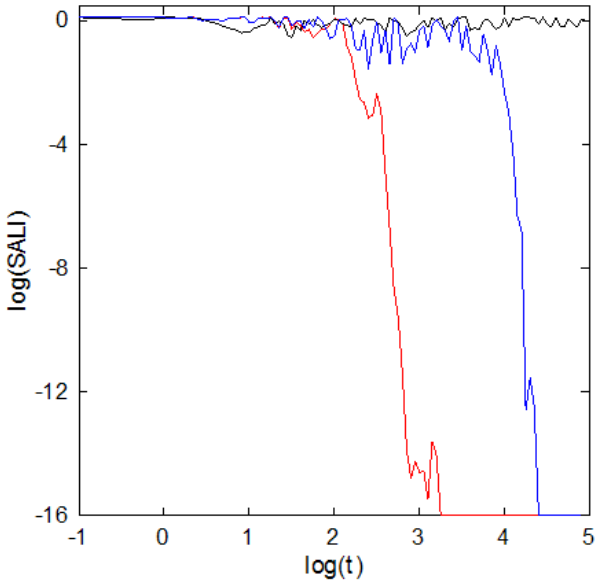

# SALI – Hénon-Heiles system

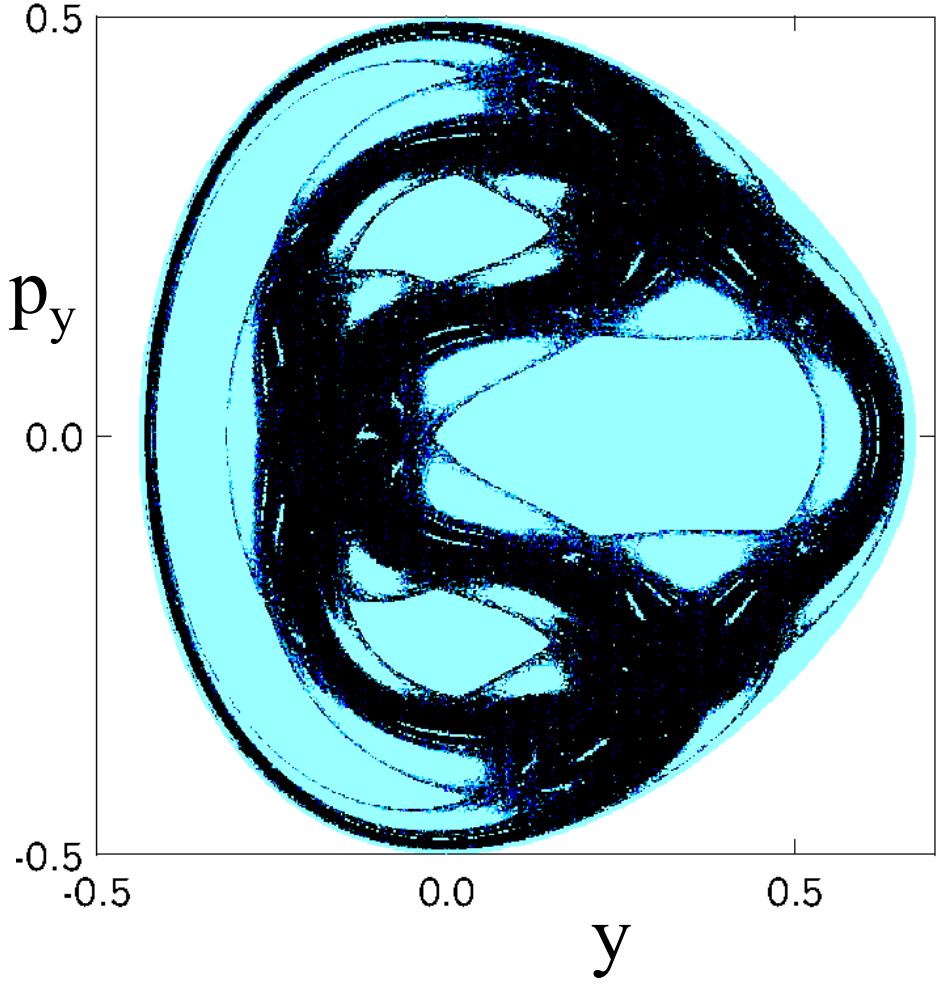


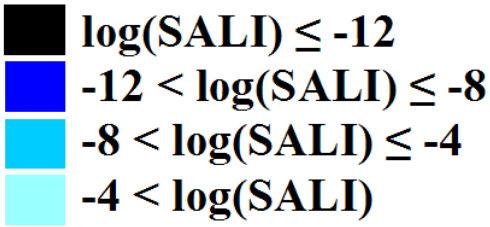

# Behavior of SALI

Hamiltonian flows and multidimensional maps

SALI→0 exponential decay for chaotic orbits

SALI→constant ≠ 0 for regular orbits

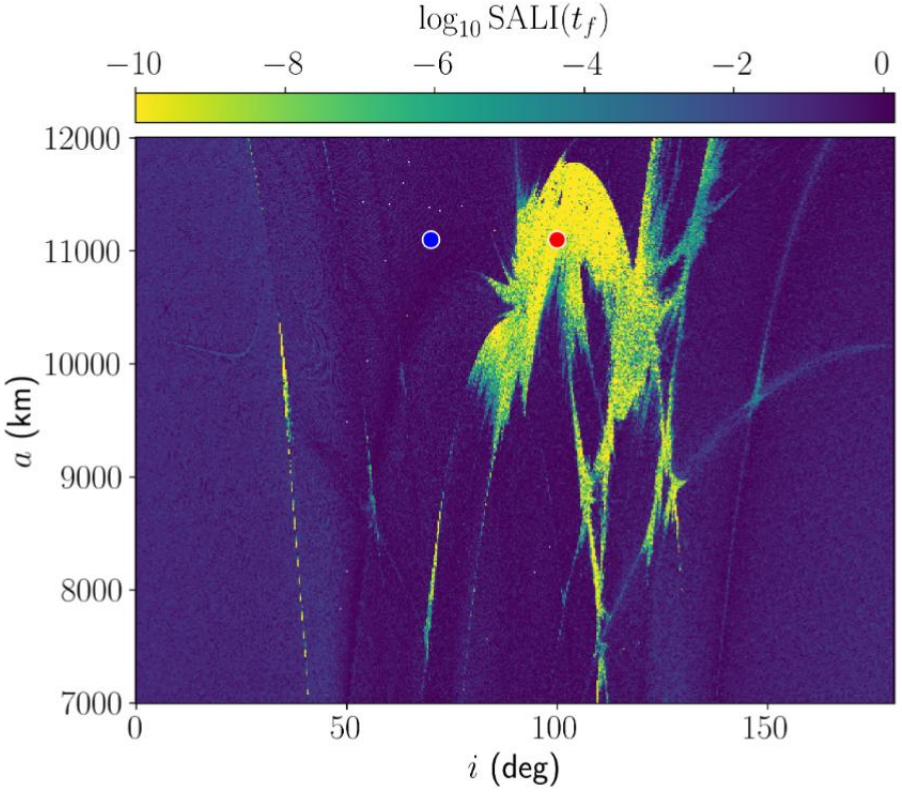


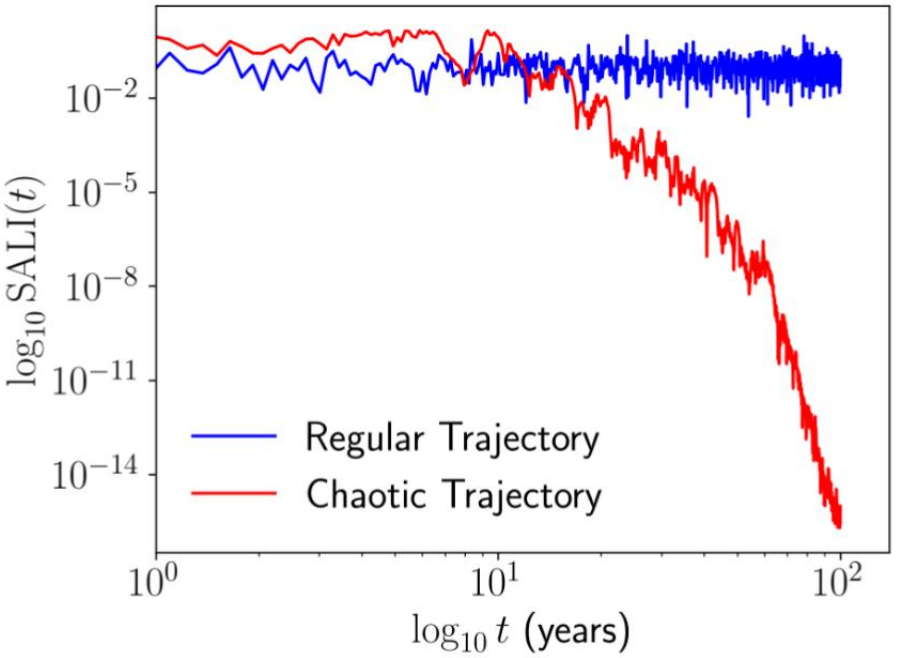


We consider initial conditions (ICs) with $e = 0.05$ and $\omega = \Omega = \lambda_\odot = 0°$, for $A/m = 10\ \mathrm{m^2 Kg^{-1}}$. We register SALI at $t_f = 100$ years.

# The effect of area-to-mass ratio

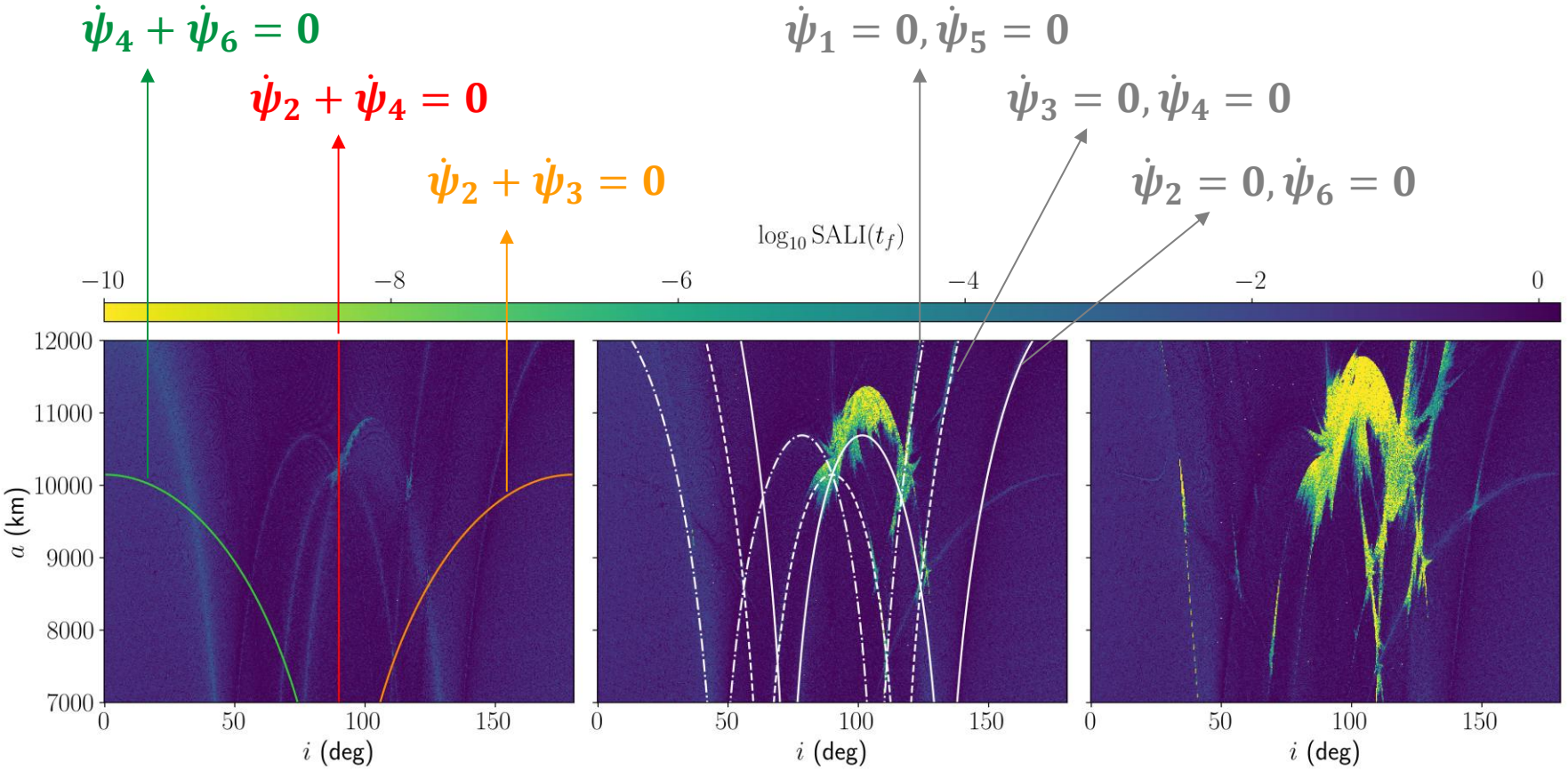


$A/m = 1\ \mathrm{m^2Kg^{-1}}$ $A/m = 5\ \mathrm{m^2Kg^{-1}}$ $A/m = 10\ \mathrm{m^2Kg^{-1}}$

We consider ICs with $e = 0.05$ and $\omega = \Omega = \lambda_{\odot} = 0°$ and register SALI at $t_f = 100$ years. Resonances are computed by considering only the Earth's oblateness perturbation.

# Orbital lifetime and re-entry trajectories

Orbital lifetime $t_*$: the time an orbit with initial semi-major axis $a_0$ needs to reach the critical eccentricity $e_* = 1 - \frac{r_E+\delta}{a_0}$ ($r_E = 6378.1363$Km and $\delta = 120$Km). At that time the orbit is considered a re-entry trajectory.

$$N_* \sim t_*^{-2}$$

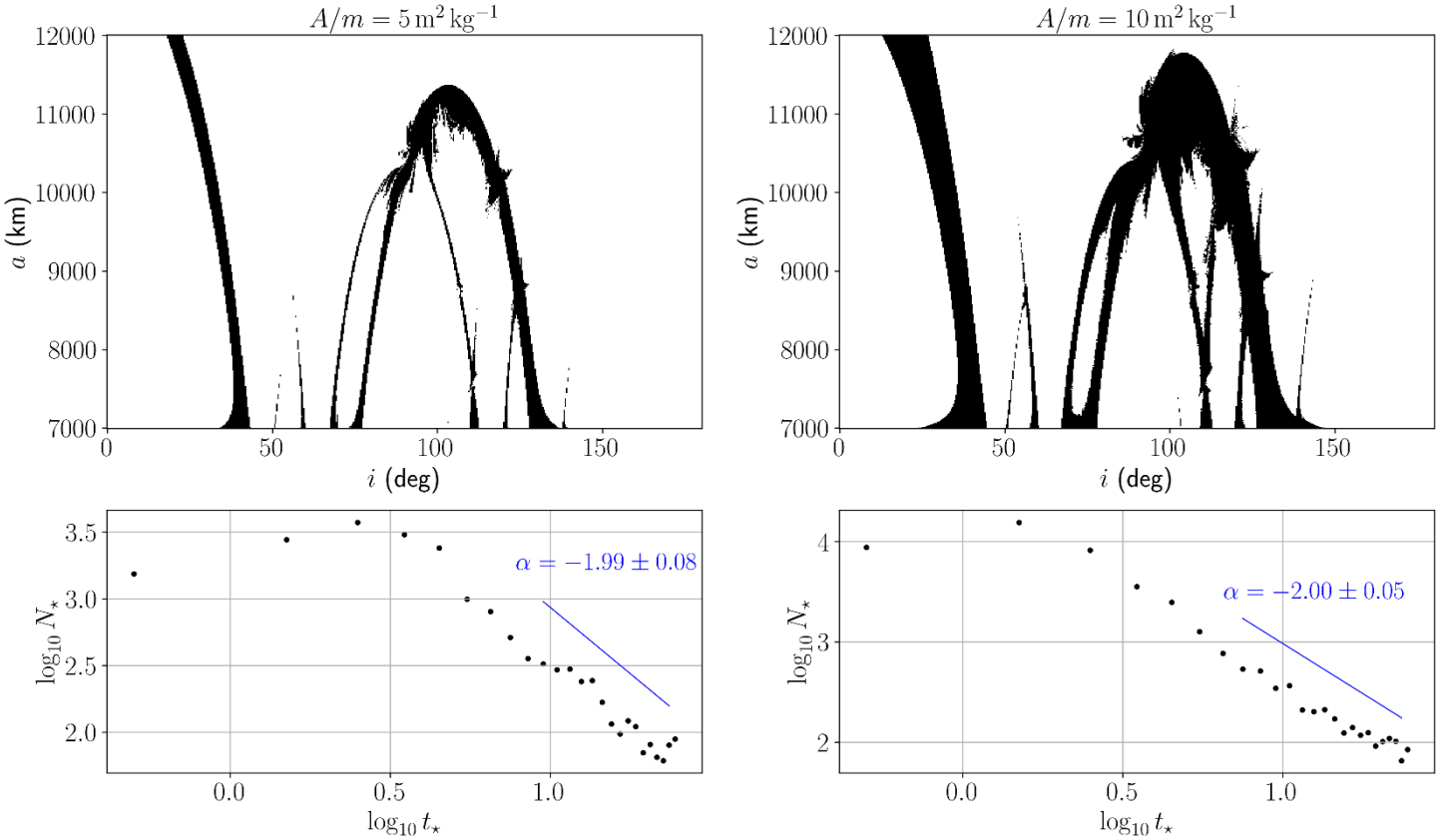


$N_*$: the number of ICs (out of about 260,000 considered orbits) leading to re-entry for times less than 25 years.

# Chaoticity and orbital lifetimes

Note that SALI is computed at the orbital lifetime $t_*$ of each trajectory.

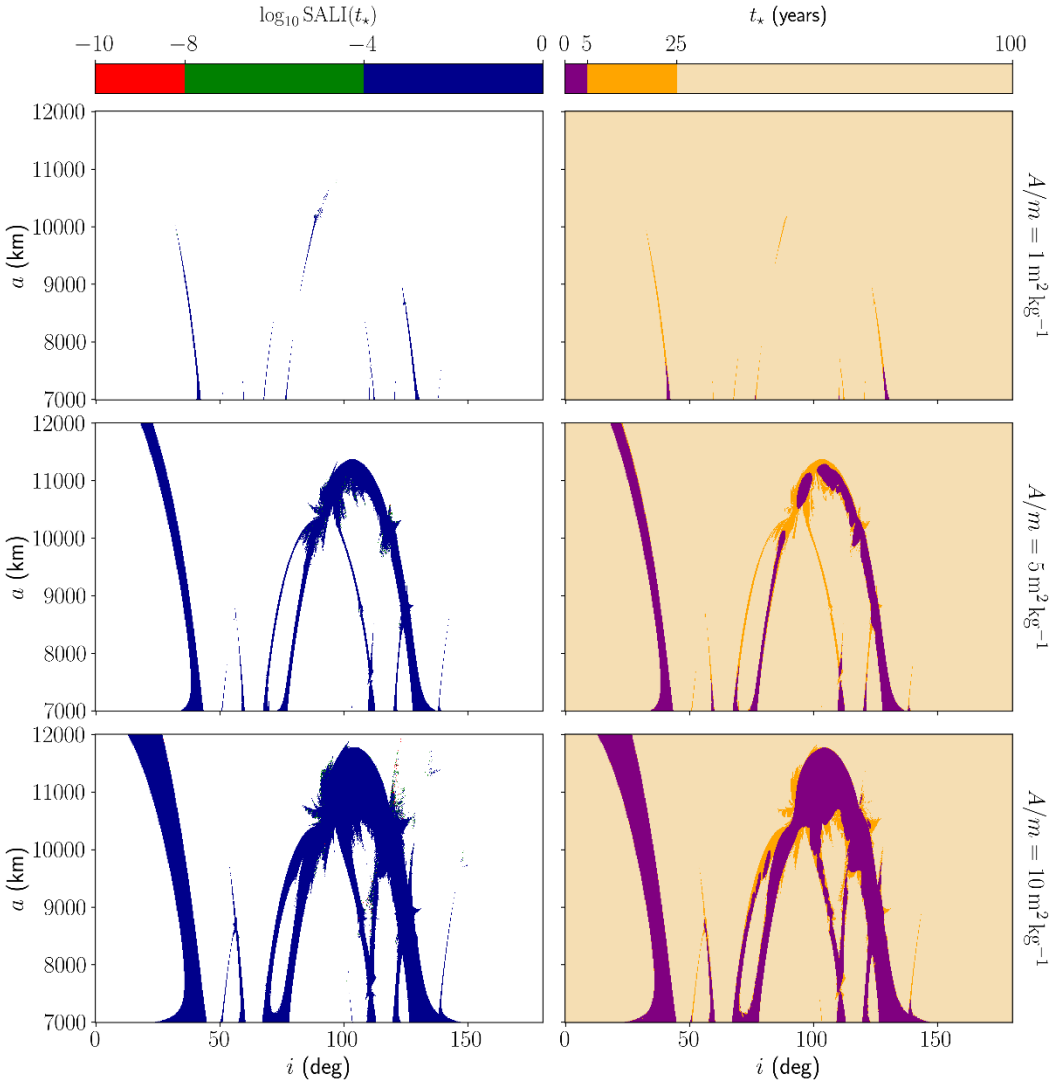


Almost all re-entry trajectories, at both $t_* = 5$ or $t_* = 25$ years, exhibit regular behavior until the time of re-entry.

# Chaoticity and orbital lifetimes

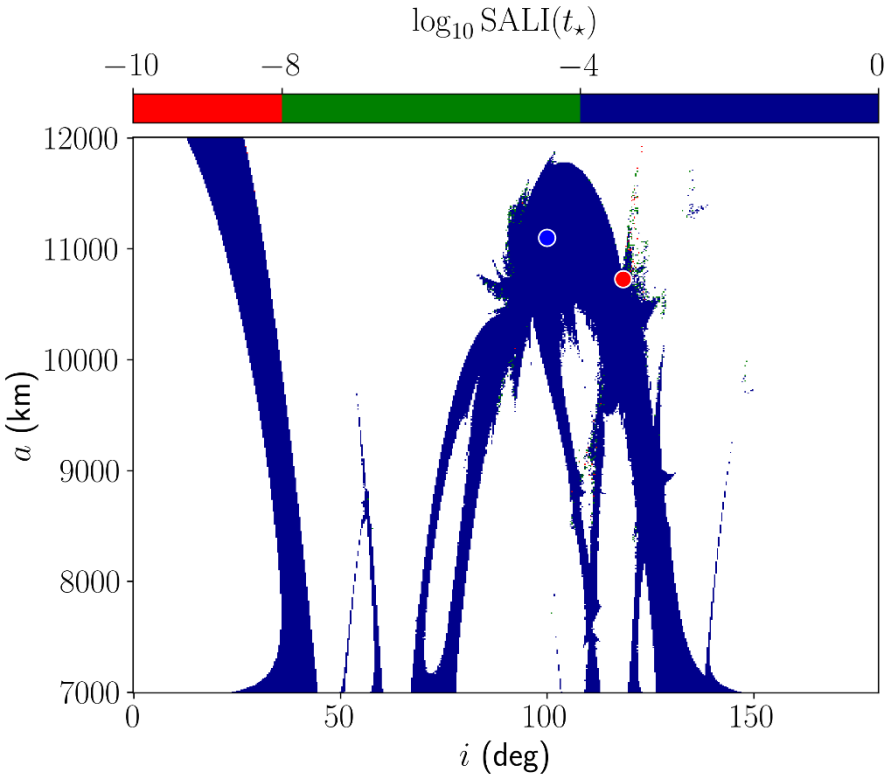


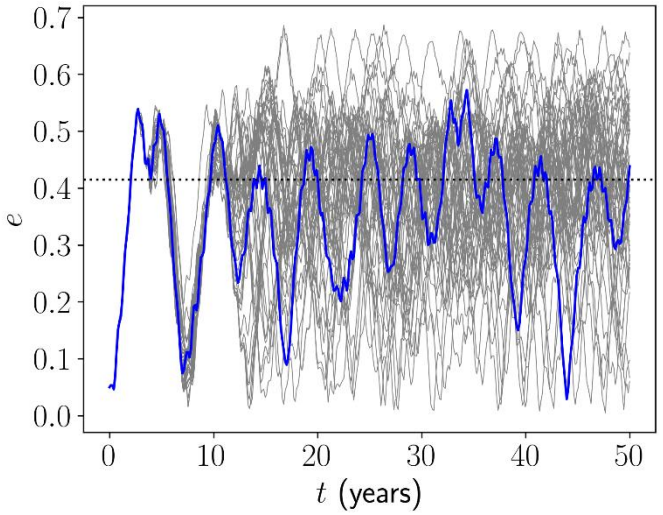


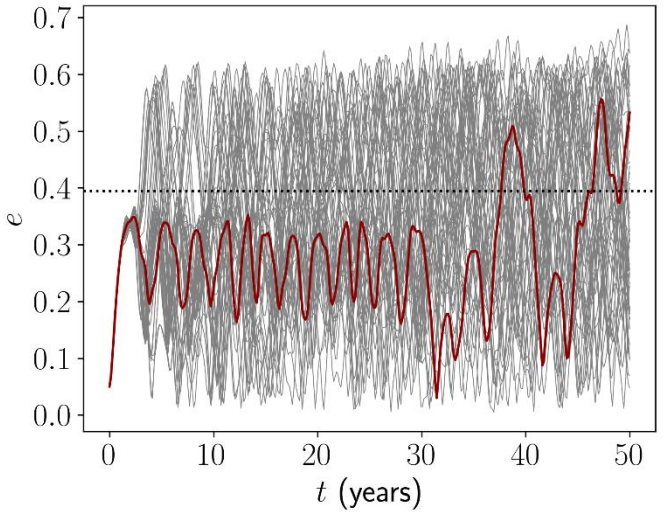


$(a, e, i, \omega, \Omega) = (11100\mathrm{Km}, 0.05, 100°, 0°, 0°)$

$(a, e, i, \omega, \Omega) = (10727.98\mathrm{Km}, 0.05, 118.36°, 0°, 0°)$

We consider 50 randomly generated ICs (grey curves) within the neighborhood of the nominal orbit.

# Summary

- We conducted a numerical investigation of Earth satellite orbital dynamics under perturbations to the two-body Kepler problem arising from solar radiation pressure and the Earth's oblateness.
- The Smaller ALignment Index method (SALI) allows the fast and clear identification of chaotic regions.
- The number $N_*$ of re-entry trajectories follows a power law decay with respect to the orbital lifetime $t_*$: $N_* \sim \frac{1}{t_*^2}$.
- Almost all re-entry trajectories (at both $t_* = 5$ or $t_* = 25$ years) exhibit regular behavior until the time of re-entry.

**References**


Alessi, Schettino, Rossi & Valsecchi (2018) MNRAS, 473, 2407
Benettin, Galgani & Strelcyn (1976) Phys. Rev. A, 14, 2338
Gkolias, Alessi & Colombo (2020) Celest. Mech. Dyn. Astron., 132, 55
S. (2001) J. Phys. A, 34, 10029
S. & Manos (2016) Lect. Notes Phys., 915, 129
S., Antonopoulos, Bountis & Vrahatis (2004) J. Phys. A, 37, 6269